ORGANIC CHEMISTRY FRONTIERS

RESEARCH ARTICLE

View Article Online
View Journal | View Issue

Cite this: *Org. Chem. Front.*, 2024, **11**, 2922

Triazatriangulenium salts – hosts and guests in supramolecular assemblies in solution†

Sayan Sarkar, Michael Böck, Agnes Uhl, Aleksandr Agafontsev, Jürgen Schatz * and Evgeny A. Kataev *

Received 18th March 2024,
Accepted 2nd April 2024

DOI: 10.1039/d4qo00500g

rsc.li/frontiers-organic

Self-assembly of triazatriangulenium dyes (TATA) bearing C3-C8 substituents and their interaction with aromatic compounds were studied. The dyes with alkyl chains longer than C5 were strongly aggregated in solution, while those with shorter alkyl chains formed hetero-stacks with aromatic compounds in chloroform. Anthracene, pyrene, coronene, and a naphthalene diimide dye formed heterostacks in solution with association constants 10^4 M^{-1}. Anthracene and pyrene-based water-soluble cyclophanes were designed to investigate host–guest complexes with TATA dyes in an aqueous solution. Experimental and theoretical investigations suggest that only pyrene-based cyclophane is able to encapsulate TATA dyes. These self-assembled structures constitute new supramolecular motifs to construct multilayered organic structures.

Introduction

Triangulenium salts are suitable platforms for constructing fluorescent dyes,[1,2] which are utilized as building blocks for controlled self-assembly,[3] imaging,[4] and catalysis.[5] Owing to their excellent stability and photophysical properties, these dyes are promising platforms for the formation of self-assembled monolayers and aggregates with aromatic compounds.[6] By organizing several molecules into complex structures in a columnar stacking way,[7] we could generate properties that open the way for developing new organic electronic materials like transistors, molecular wires, and solar cells.[7,8] Moreover, the heterostacks are highly attractive in terms of stabilization of radical species.[9,10]

For example, the self-assembly of triangulenium dyes has been observed in solution[11–13] and in the solid state,[14] featuring columnar or lamellar architectures. The overall self-assembled structures and their fluorescent properties depend on the alkyl chain length attached at different positions and the nature of the couteranion.[15–18] Moreover, these dyes can form heterostacks with other fluorescent dyes showing bright fluorescence emission.[4,7,19–21] However, there is still a gap in understanding how TATA dyes interact with various π-systems in solution and how strong the interactions are.

TATA dyes can potentially interact with other aromatic compounds and form ordered architectures. Knowing how dyes interact in solution with each other is very important for understanding and controlling the self-assembly processes of formed aggregates. Toward this goal, we have prepared triazatriangulenium dyes bearing alkyl chains of different lengths and studied their self-assembly behavior in organic and aqueous solutions with selected aromatic compounds and water-soluble cyclophanes. We show that TATA dyes with alkyl chains shorter than C6 are prone to form heterostacks with aromatic compounds in chloroform. In contrast, the dyes bearing C6 and longer chains tend to show a substantial degree of aggregation. We also found that the dyes can be encapsulated into the pyrene-based cyclophane in an aqueous solution, producing pyrene-TATA-pyrene heterostacks.

Results and discussion

Synthesis and self-aggregation properties

TATA dyes bearing alkyl chains C3, C4, C5, C6, and C8 were synthesized as tetrafluoroborate salts using the procedure reported by Laursen and coworkers.[22,23] The reported crystallographic data suggest several possible self-assembly modes for the dyes in the solid state. TATA dyes form staggered cationic dimers if the alkyl substituents are short. Lengthening the alkyl chains breaks the symmetry of self-assembled architectures. For example, propyl groups are on the plane of the rings, while octyl groups are located perpendicular to the aromatic rings (Fig. 1). Such an organization can also be expected in the solution. Our preliminary UV-Vis dilution experiments evidenced the self-aggregation of all obtained compounds in $CHCl_3$ at concentrations higher than 10^{-4} M. We measured the fluorescence intensity of the dyes dependent on their concen-

Friedrich-Alexander Universität Erlangen-Nürnberg, Department of Chemistry and Pharmacy, Nikolaus-Fiebiger-Strasse 10, 91058 Erlangen, Germany.
E-mail: evgeny.kataev@fau.de, juergen.schatz@fau.de

† Electronic supplementary information (ESI) available. See DOI: https://doi.org/10.1039/d4qo00500g

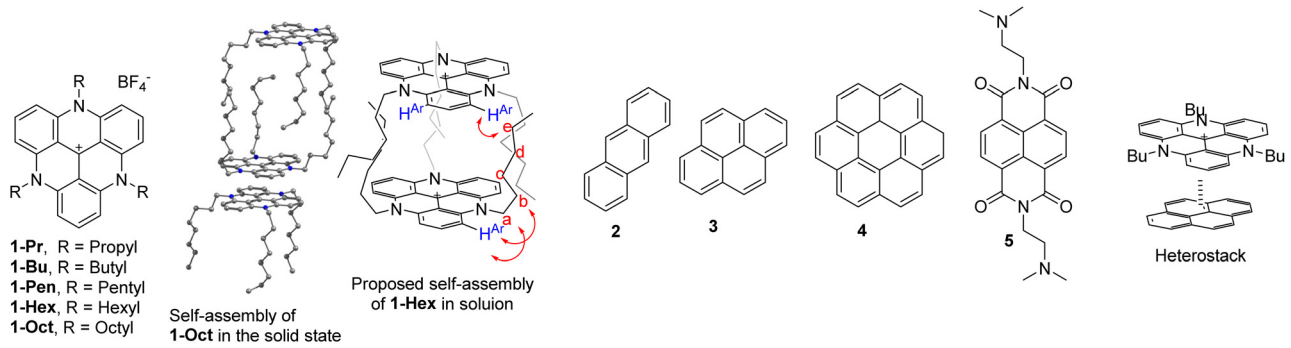

Fig. 1 Structures of investigated compounds. Snapshot of **1-Oct** self-assembly in the solid state according to the X-ray data[22] and the proposed mode of aggregation based on ROESY experiment for **1-Hex**. Structures of **2–5** and proposed interaction mode in solution of **1-Bu** with pyrene.

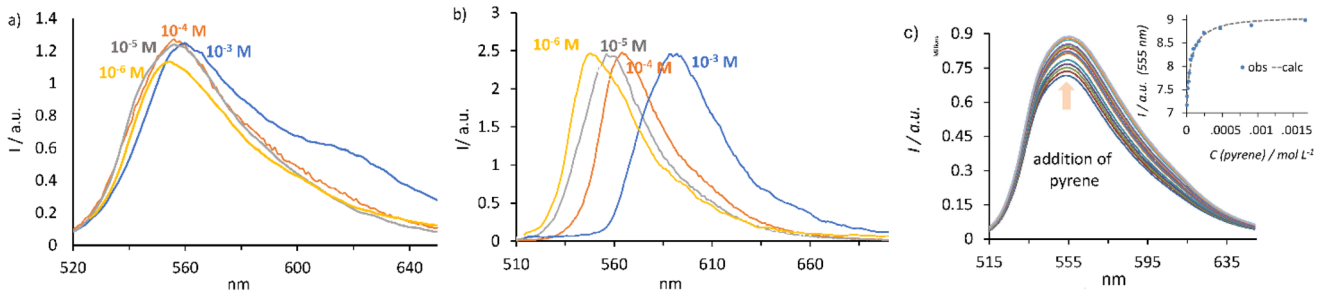

Fig. 2 Normalized emission spectra of TATA salts after correction for inner-filter effect: (a) **1-Bu** and (b) **1-Hex** at different concentrations in $CHCl_3$. (c) Fluorescence titration of **1-Bu** with pyrene and the corresponding fitting curve.

tration in $CHCl_3$, and temperature-dependent spectra at different concentrations covering the range from 10^{-6} to 10^{-3} M (Fig. S9–S16, ESI†). The fluorescence spectra at higher concentrations were corrected for the inner-filter effect,[24,25] according to the known procedure.[26] As can be seen in Fig. 2a and b, the emission maximum of **1-Bu** does not change much at different concentrations, while that for **1-Hex** undergoes a bathochromic shift upon increasing the concentration toward 10^{-3} M. The shift was not observed for the dyes with shorter hydrocarbon chains than four carbon atoms. The UV-Vis temperature-dependent investigations for **1-Hex** and **1-Oct** show a characteristic increase in the band absorption at 525 nm, while **1-Pr**, **1-Bu**, and **1-Pen** absorption gradually increase upon heating from 0 °C to 50 °C. These experiments suggest the presence of **1-Hex** and **1-Oct** in chloroform solution in the aggregated state (Fig. S23†).

Additional evidence of efficient self-assembly of TATA dyes in chloroform was obtained by analyzing the ^1H–^1H ROESY spectra. Several correlations were found for **1-Hex** and **1-Oct** between H^{Ar} and protons H^a–H^g in the alkyl chain, while for **1-Bu**, only correlation with H^a and H^b were detected (Fig. S35†). The correlations with distant H^e–H^g are possible in the aggregate with a structure similar to that found in the solid state (Fig. 1).[22,27]

Interaction with aromatic compounds

The interaction of TATA dyes with polycyclic aromatic compounds (anthracene (**2**), pyrene (**3**), coronene (**4**), and NDI (**5**)) was investigated at 10^{-5}–10^{-6} M concentration by fluorescence and UV-Vis spectroscopy in $CHCl_3$ (Fig. 2c, Fig. S21 and S22†). These polycyclic aromatic compounds were chosen because their absorption does not overlap with the absorption of TATA dyes (Fig. S20†). Therefore, TATA dyes could be selectively excited at 500 nm. The emission at 560 nm was recorded upon increasing the concentration of the interacting partners 2–5. The binding constants and stoichiometry were obtained by fitting the whole spectrum with HypSpec and HypNMR programs.[28,29] As can be inferred from Table 1, the 1 : 1 complexes are stable in solution with the highest binding constants observed for the **1-Bu** dye and reaching 10^4 M^{-1}. However, there is no considerable selectivity to one of the investigated aromatic compounds. Coronene demonstrated

Table 1 Association constants (log *K*) of TATA dyes determined by using fluorescence and UV-Vis titrations in $CHCl_3$. Standard deviations are shown in parentheses

Dye	1-Pr		1-Bu	
	Fluorescence	UV-Vis	Fluorescence	UV-Vis
Anthracene(**2**)	3.47(3)	3.69(2)	4.18(4)	4.12(2)
Pyrene(**3**)	3.65(2)	3.98(2)	4.18(4)	3.72(2)
Coronene(**4**)	[a]	3.00(2)	3.52(3)	[a]
NDI(**5**)	3.26(1)	3.51(1)	4.15(5)/	4.01(2)

[a] Small changes were observed.

lowest binding affinities, likely because steric interactions with alkyl substituents. All the aromatic compounds induced a fluorescence increase.

Surprisingly, very small or no changes in fluorescence were detected with TATA dyes bearing pentyl, hexyl and octyl substituents. Likely, the aggregation of these dyes in chloroform occurs even at 10^{-6} M concentration and lower, which hampers interaction with other dyes in solution. Electrospray ionization mass studies revealed the presence of a 1 : 1 complex between **1-Bu** and pyrene at *m*/*z* 650.35, corresponding to adduct [**1-Bu**·Pyrene-2*H*] (Fig. S37†). We suggested that **1-Bu** forms a radical species in the gas phase, which reacts with pyrene, connecting the interacting species with a covalent bond. Similar reactivity was observed previously for TATA dyes during electrochemical studies.[30]

Interaction with cyclophanes

Supramolecular architectures formed *via* aggregation attract considerable attention due to their potential application in light-emitting diodes and solar cells.[8] The self-assembly of different dyes in an aqueous solution is less explored.[31,32] TATA dyes possess a large surface area, and thus, they are prone to form strong dispersion interactions. These interactions can be maximized in an aqueous solution.[33–35] To understand noncovalent interactions between TATA dyes and polycyclic compounds in water, we developed water-soluble macrocycles **6** and **7**, bearing anthracene and pyrene subunits, respectively (Fig. 3). We found that acetonitrile–water solvent mixtures are suitable for solubilizing TATA dyes and macrocycles and thus allowed us to investigate their interaction. Macrocycles **6** and **7** are water-soluble and negatively-charged analogs of the receptors recently developed by us. They feature a bellows-type sensing mechanism realized to detect ATP.[36]

First, we studied the interaction of **6** and **7** with TATA dyes in a 1% CH_3CN in a 50 mM MOPSO buffer (pH 7.4). Only **1-Pr** and **1-Bu** do not aggregate in this solution at a concentration 10^{-6} M, as confirmed by the dilution experiments (Fig. S11†). The spectra obtained at 350 nm excitation revealed that macrocycles were found in an equilibrium of the stacked and the open forms in solution, which are responsible for the excimer and monomer bands, respectively (Fig. 3). The strong excimer band for **7** suggests that the stacked form is predominant in the solution. The equilibrium between the stacked and open forms depends on pH. The stacked form prevails at basic pH (7.4), while the open is favorable at acidic pH (5.2). This behavior was evidenced by the bathochromic shift in UV-Vis spectra and the high intensity of the excimer band in the fluorescence spectrum (Fig. S30†). The UV-Vis data confirms that the equilibrium between the open and the stacked forms occurred also in the ground state (Fig. S33†).

We suggested that TATA dyes can either interact with the stacked form of the macrocycle (coordination on top) or be located between the aromatic rings in the cyclophane (encapsulation, Fig. 3). Static quenching and the formation of the supramolecular complexes between the macrocycles and TATA dyes was evident from non-linear Sterm–Volmer plots. Due to

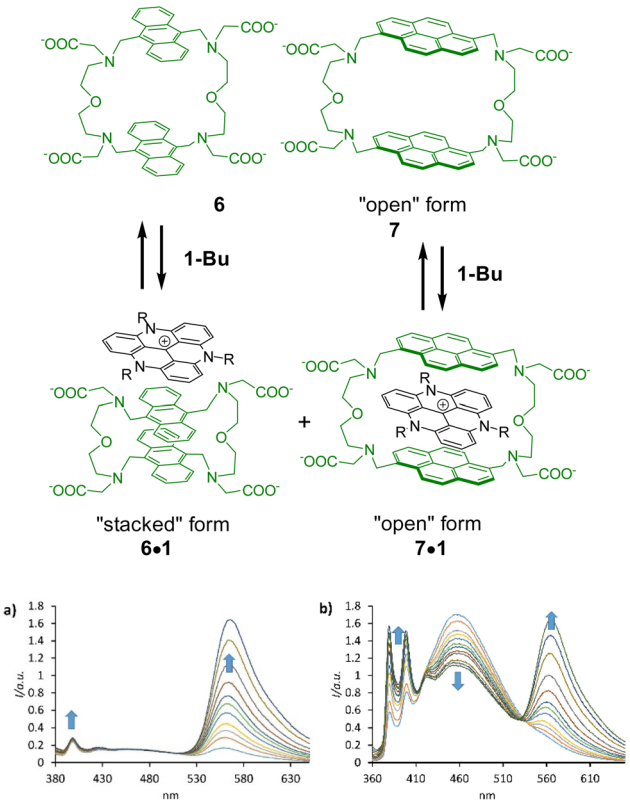

Fig. 3 Structure of pyrene- and anthracene-containing macrocycles and proposed binding modes of **7** with **1-Bu**. Fluorescence spectra of (a) **6** and (b) **7** (ex. 350 nm) observed by the addition of **1-Bu** to the solution of macrocycles. Condition: 10^{-6} M receptor, 1% CH_3CN, 50 mM MOPSO buffer, pH 7.4.

the complex dissociation at higher temperatures, the quenching efficiency drops considerably (Fig. S31†). This fact additionally proves the static nature of quenching.

To elucidate the interaction modes in the supramolecular complex, we performed fluorescence titration of macrocycles with **1-Bu** (ex. 350 nm) and obtained binding constants $\log K$ = 5.1(3) for **6** and $\log K$ = 5.6(3) for **7**, respectively (Fig. S26–S29†). The results of the reverse titrations of TATA dyes (**1-Bu** and **1-Pr**) excited at 500 nm with macrocycles **6** and **7** were in agreement with the previous method: complex **6·1-Bu** has $\log K$ = 5.3(2); complex **7·1-Bu** – $\log K$ = 5.4(2); complex **6·1-Pr** – $\log K$ = 4.9(1); complex **7·1-Pr** – $\log K$ = 5.0(1). The fluorescence titration with excitation at 350 nm provided valuable information on how excimer and monomer bands of pyrene were changed in the presence of dyes. For instance, adding **1-Bu** to the anthracene macrocycle (**6**) did not substantially change the excimer emission. However, upon titration of receptor **7** with **1-Bu** (or **1-Pr**), a considerable decrease in the excimer emission band and an increase in the monomer emission band were observed. Moreover, the emission of **1-Bu** at 564 nm undergoes a 10 nm bathochromic shift. This result suggests the possible encapsulation of the TATA dye between two pyrene rings. Time-resolved fluorescence measurements were conducted for **7** with increasing concentrations of **1-Bu** (up to 20 equiv.). In

this case, the lifetimes of the excimer band decreased upon the addition of the TATA dye (4.22 to 4.05 ns) (Fig. S32†). These results perfectly agree with the time-resolved studies for the previously reported acyclic bis-pyrene receptor.[37] Based on our data, we proposed that the 'encapsulation' binding mode for the pyrene-based cyclophane might be predominant, while anthracene cyclophane might show both interaction modes.

Further support for binding events with **7** was obtained by ^{1}H NMR measurements. Since the NMR method required higher concentrations of the reagents, we used a 1 : 1 CH_3CN-buffer mixture as a solvent. According to the dilution experiments, TATA dyes show evidence of weak aggregation at 10^{-3} M concentration. Two proton signals of the triangulenium core underwent upfield shift upon the addition of the macrocycle **7** to **1-Bu**, while the signals of the macrocycle shift to the low field (Fig. 4a). The shifts of both host and guest complexes provide solid evidence that the interaction occurs even under these conditions. The experimental data (proton shifts) were successfully fitted to a mixed binding event – dimerization of the TATA dyes and 1 : 1 complex formation with macrocycle **7** (Fig. 4b). The dimerization ($\log K_d$) and binding constants ($\log K_a$) for **1-Pr** and **1-Bu** have the following values: $\log K_d$ = 3.52(1) and $\log K_a$ = 3.34(2), $\log K_d$ = 3.32 and $\log K_a$ = 2.84, respectively (Fig. 4a and Fig. S36, ESI†). Slightly lower binding constants observed for **1-Bu** can be explained by the higher bulkiness of the butyl group.

Electrospray ionization of host–guest complexes dissolved in acetonitrile–water solution revealed the formation of a 1 : 1 complex of the macrocycles with TATA dyes (Fig. 4c). The formation of complexes was detected for both macrocycles **6** and **7** (Fig. 4c). The composition of complexes was the dianionic

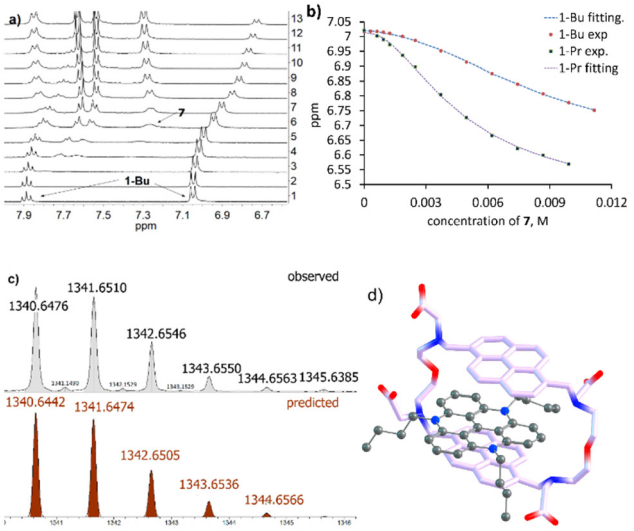

Fig. 4 (a) ^{1}H NMR titration of **1-Bu** with **7** in a 1 : 1 CD_3CN-buffer mixture (1 mM of **1-Bu**, addition of **7** to **1-Bu**, 50 mM MOPSO in D_2O, pH 7.4). (b) Observed chemical shifts and fitting curves for the NMR titrations with **1-Pr** and **1-Bu**. (c) ESI-MS of **7** with **1-Bu**, calculated and observed isotope distribution. (d) DFT optimized molecular structure of the complex [**7**·**1-Bu**]$^{3-}$; hydrogen atoms were omitted for clarity.

macrocycles complexed with the triazatriangulenium cation: *m*/*z* 1292.64 for [**6**-2H + **1-Bu**$^+$]$^-$ and *m*/*z* 1340.64 for [**7**-2H + **1-Bu**$^+$]$^-$.

The structure of the host–guest complex [**7**·**1-Bu**]$^{3-}$ was elucidated with the help of DFT calculations. The calculations were performed at the BP86-def2-TZVP level of theory with a D3 model for dispersion corrections[38] by using ORCA Software package.[39] The resulting structure is shown in Fig. 4d. Triazatriangulenium cation is ideally located between two pyrene rings with a distance of 3.21 Å to pyrenes and is stabilized through dispersion interactions. The butyl groups are too large to allow the dye to achieve maximum surface overlap with pyrenes.

Conclusions

In summary, we have investigated the self-assembly and recognition properties of TATA dyes bearing alkyl chains of different lengths. We have found that starting from pentyl substituents and longer, the dyes undergo strong aggregation in chloroform even at concentrations less than 10^{-5} M. The dyes with shorter chains are able to form hetero-stacks with aromatic guests showing association constants around 10^4 M^{-1}. Water-soluble anthracene and pyrene-based cyclophanes have been designed to investigate the interaction with TATA dyes in an aqueous solution. The results show that **7** can strongly interact with dyes, forming triple hetero-stacks with binding constants reaching 10^5 M^{-1}. These self-assembled structures constitute new supramolecular motifs for constructing more complex architectures, such as interlocked molecules or multilayered organic structures. TATA dyes are known to form radicals under light excitation or reductive conditions. Encapsulation of TATA dyes by cyclophanes is an attractive way to investigate the supramolecular stabilization of radical species. The work along this line is currently in progress.

Experimental section

General methods

All the starting materials and compounds **2**, **3** and **4** were purchased from commercial sources such as Sigma Aldrich, Fischer Sci, and TCI; they are used as received without further purification. All solvents were purified by distillation using a rotary evaporator. The triangulenium salts (**1-Pr**, **1-Bu**, **1-Pen**, **1-Hex** and **1-Oct**) were synthesized following literature known procedures.[22] All reaction mixtures were stirred magnetically. For dryness of the products, a vacuum system consisting of a cold trap linked to an oil pump (OERLIKON LEYBOLD VACUUM Trivac) was used. An ultimate vacuum of 10^{-3} mbar could be achieved. Electrospray ionization mass spectroscopy (ESI-MS) experiments were carried out on SHIMADZU BIOTECH AXIMA Confidence in positive and negative ion ESI mode. Absorption spectra were recorded in 1 cm quartz cuvettes (Hellma) on a VARIAN Cary 6000 and Cary 50 spec-

trometers. Emission spectra were recorded in 1 cm quartz cuvettes (Hellma) on a FluoroMax PLUS (Horiba) with temperature control. Fluorescence binding constants were calculated using hypspec software. All the NMR experiments were obtained on 300, 400, and 600 MHz Bruker Avance.

Synthesis of 7

The pyrene-based cyclophane synthesized by us previously[36] (84 mg, 0.127 mmol), KI (84 mg, 0.504 mmol), potassium carbonate (141 mg, 1 mmol, 8 equiv.) and ethylchloroacetate (93 mg, 0.763 mmol, 6 equiv.) were placed in a flask containing 50 mg of THF. The reaction mixture was heated to 60 °C under nitrogen atmosphere for 40 h, until the starting macrocycle disappears on TLC. The solvent was removed, water added, and the mixture was extracted with chloroform. The product was purified by column chromatography in DCM-EtOAc 3 : 1 mixture. The product was dissolved in 10 ml THF and 5 ml of EtOH. To this solution, NaOH (39.8 mg, 0.995 mmol, 10 equiv.) was added and stirred for 1 h. The formed precipitated was filtered off. Yellow solid (Yield 80%). ^{1}H NMR (600 MHz, DMSO-d_6) δ 8.27 (brs, 4H), 7.74 (s, 4H), 7.59 (d, J = 7.6 Hz, 4H), 7.49 (d, J = 7.6 Hz, 4H), 7.17 (s, 4H), 3.90 (s, 8H), 3.56 (t, J = 5.2 Hz, 8H), 2.94–2.71 (m, 16H). ^{13}C (^{1}H) NMR (DMSO-d_6) δ 177.3, 133.6, 130.0, 128.9, 127.3, 126.7, 124.8, 124.5, 122.6, 55.1, 52.0, 49.3, 48.8 HRMS (ESI-TOF) m/z calcd for $C_{52}H_{51}N_4O_{10}^-$ 891.3605. Found: $[M - H]^-$ 891.3627.

Synthesis of 6

The synthesis was performed according to the method described for bis-pyrene macrocycle 7. The starting anthracene cyclophane was prepared as described earlier.[40] The product also precipitated from the solution as a pure compound. Yellow solid (Yield 81%). ^{1}H NMR (400 MHz, DMSO-d_6–D_2O 5 : 1) δ 8.44–8.34 (m, 8H), 7.14 (dd, J = 7.1, 3.2 Hz, 8H), 4.23 (s, 8H), 3.12 (brs, 8H), 2.90 (s, 8H), 2.55 (t, J = 6.0 Hz, 8H). ^{13}C (^{1}H) NMR (DMSO-d_6–D_2O 5 : 1) δ 177.0, 131.7, 131.5, 126.5, 125.7, 68.1, 59.0, 52.6, 51.0. HRMS (ESI-TOF) m/z calcd for $C_{48}H_{51}N_4O_{10}^-$ 843.3611. Found: $[M - H]^-$ 843.3626.

Conflicts of interest

The authors declare no conflict of interests.

Acknowledgements

J. S. and E. A. K. gratefully acknowledge financial support from Deutsche Forschungsgemeinschaft Grant KA3444/16-1 and Collaborative Research Centre SFB 953.

References

1 J. Bosson, J. Gouin and J. Lacour, Cationic triangulenes and helicenes: synthesis, chemical stability, optical properties and extended applications of these unusual dyes, *Chem. Soc. Rev.*, 2014, **43**, 2824–2840.
2 B. W. Laursen and F. C. Krebs, Synthesis of a triazatriangulenium salt, *Angew. Chem., Int. Ed.*, 2000, **39**, 3432–3434.
3 B. Dong and H. Maeda, Ion-based materials comprising planar charged species, *Chem. Commun.*, 2013, **49**, 4085–4099.
4 L. Kacenauskaite, N. Bisballe, R. Mucci, M. Santella, T. Pullerits, J. Chen, T. Vosch and B. W. Laursen, Rational Design of Bright Long Fluorescence Lifetime Dyad Fluorophores for Single Molecule Imaging and Detection, *J. Am. Chem. Soc.*, 2021, **143**, 1377–1385.
5 C. Nicolas and J. Lacour, Triazatriangulenium Cations: Highly Stable Carbocations for Phase-Transfer Catalysis, *Org. Lett.*, 2006, **8**, 4343–4346.
6 M. Hardouin-Lerouge, P. Hudhomme and M. Sallé, Molecular clips and tweezers hosting neutral guests, *Chem. Soc. Rev.*, 2011, **40**, 30–43.
7 B. Qiao, B. E. Hirsch, S. Lee, M. Pink, C.-H. Chen, B. W. Laursen and A. H. Flood, Ion-Pair Oligomerization of Chromogenic Triangulenium Cations with Cyanostar-Modified Anions That Controls Emission in Hierarchical Materials, *J. Am. Chem. Soc.*, 2017, **139**, 6226–6233.
8 D. Bialas, E. Kirchner, M. I. S. Rohr and F. Wurthner, Perspectives in Dye Chemistry: A Rational Approach toward Functional Materials by Understanding the Aggregate State, *J. Am. Chem. Soc.*, 2021, **143**, 4500–4518.
9 T. Y. Jiao, K. Cai, J. N. Nelson, Y. Jiao, Y. Y. Qiu, G. C. Wu, J. W. Zhou, C. Y. Cheng, D. K. Shen, Y. N. Feng, Z. C. Liu, M. R. Wasielewski, J. F. Stoddart and H. Li, Stabilizing the Naphthalenediimide Radical within a Tetracationic Cyclophane, *J. Am. Chem. Soc.*, 2019, **141**, 16915–16922.
10 A. Trabolsi, N. Khashab, A. C. Fahrenbach, D. C. Friedman, M. T. Colvin, K. K. Coti, D. Benitez, E. Tkatchouk, J. C. Olsen, M. E. Belowich, R. Carmielli, H. A. Khatib, W. A. Goddard, M. R. Wasielewski and J. F. Stoddart, Radically enhanced molecular recognition, *Nat. Chem.*, 2010, **2**, 42–49.
11 A. Winter and U. S. Schubert, The supramolecular assemblies based on heteroatom-containing triangulenes, *Mater. Chem. Front.*, 2019, **3**, 2308–2325.
12 F. Westerlund, J. Elm, J. Lykkebo, N. Carlsson, E. Thyrhaug, B. Åkerman, T. J. Sorensen, K. V. Mikkelsen and B. W. Laursen, Direct probing of ion pair formation using a symmetric triangulenium dye, *Photochem. Photobiol. Sci.*, 2011, **10**, 1963–1973.
13 B. W. Laursen, J. Reynisson, K. V. Mikkelsen, K. Bechgaard and N. Harrit, 2,6,10-tris(dialkylamino)trioxatriangulenium salts: a new promising fluorophore. Ion-pair formation and aggregation in non-polar solvents, *Photochem. Photobiol. Sci.*, 2005, **4**, 568–576.
14 F. Westerlund, H. T. Lemke, T. Hassenkam, J. B. Simonsen and B. W. Laursen, Self-Assembly and Near Perfect Macroscopic Alignment of Fluorescent Triangulenium Salt in Spin-Cast Thin Films on PTFE, *Langmuir*, 2013, **29**, 6728–6736.

15 H. Noguchi, T. Hirose, S. Yokoyama and K. Matsuda, Fluorescence behavior of 2,6,10-trisubstituted 4,8,12-triazatriangulene cations in solution and in the solid state, *CrystEngComm*, 2016, **18**, 7377–7383.
16 T. Hirose, K. Sasatsuki, H. Noguchi, S. Yokoyama and K. Matsuda, Aggregation of 4,8,12-Triazatriangulene Cation with Amphiphilic Side Chains: Emission Properties in Solution, in Aggregates, and in the Solid State, *Chem. Lett.*, 2016, **45**, 1090–1092.
17 Y. Haketa, K. Urakawa and H. Maeda, First decade of π-electronic ion-pairing assemblies, *Mol. Syst. Des. Eng.*, 2020, **5**, 757–771.
18 Y. Haketa, S. Sasaki, N. Ohta, H. Masunaga, H. Ogawa, N. Mizuno, F. Araoka, H. Takezoe and H. Maeda, Oriented Salts: Dimension-Controlled Charge-by-Charge Assemblies from Planar Receptor–Anion Complexes, *Angew. Chem., Int. Ed.*, 2010, **49**, 10079–10083.
19 L. Kacenauskaite, S. G. Stenspil, A. H. Olsson, A. H. Flood and B. W. Laursen, Universal Concept for Bright, Organic, Solid-State Emitters-Doping of Small-Molecule Ionic Isolation Lattices with FRET, *J. Am. Chem. Soc.*, 2022, **144**(43), 19981–19989.
20 C. R. Benson, L. Kacenauskaite, K. L. VanDenburgh, W. Zhao, B. Qiao, T. Sadhukhan, M. Pink, J. S. Chen, S. Borgi, C. H. Chen, B. J. Davis, Y. C. Simon, K. Raghavachari, B. W. Laursen and A. H. Flood, Plug-and-Play Optical Materials from Fluorescent Dyes and Macrocycles, *Chem*, 2020, **6**, 1978–1997.
21 M. Yokoyama, Y. Okayasu, Y. Kobayashi, H. Tanaka, Y. Haketa and H. Maeda, Ion-Pairing Assemblies of Dithienylnitrophenol-Based π-Electronic Anions Stabilized by Intramolecular Interactions, *Org. Lett.*, 2023, **25**, 3676–3681.
22 B. W. Laursen and F. C. Krebs, Synthesis, Structure, and Properties of Azatriangulenium Salts, *Chem. – Eur. J.*, 2001, **7**, 1773–1783.
23 T. J. Sørensen, C. B. Hildebrandt, M. Glyvradal and B. W. Laursen, Synthesis, optical properties and lamellar self-organization of new N,N′,N″-trialkyl-triazatriangulenium tetrafluoroborate salts, *Dyes Pigm.*, 2013, **98**, 297–303.
24 J. Kimball, J. Chavez, L. Ceresa, E. Kitchner, Z. Nurekeyev, H. Doan, M. Szabelski, J. Borejdo, I. Gryczynski and Z. Gryczynski, On the origin and correction for inner filter effects in fluorescence Part I: primary inner filter effect-the proper approach for sample absorbance correction, *Methods Appl. Fluoresc.*, 2020, **8**, 033002.
25 L. Ceresa, J. Kimball, J. Chavez, E. Kitchner, Z. Nurekeyev, H. Doan, J. Borejdo, I. Gryczynski and Z. Gryczynski, On the origin and correction for inner filter effects in fluorescence. Part II: secondary inner filter effect -the proper use of front-face configuration for highly absorbing and scattering samples, *Methods Appl. Fluoresc.*, 2021, **9**, 035005.
26 J. R. Lakowicz, *Principles of fluorescence spectroscopy*, Springer, New York, 3rd edn, 2006.
27 T. J. Sorensen, C. B. Hildebrandt, J. Elm, J. W. Andreasen, A. O. Madsen, F. Westerlund and B. W. Laursen, Large area, soft crystalline thin films of N, N,' N″ -alkyltriazatriangulenium salts with homeotropic alignment of the discotic cores in a lamellar lattice, *J. Mater. Chem.*, 2012, **22**, 4797–4805.
28 P. Gans, A. Sabatini and A. Vacca, Investigation of equilibria in solution. Determination of equilibrium constants with the HYPERQUAD suite of programs, *Talanta*, 1996, **43**, 1739–1753.
29 F. Ulatowski, K. Dabrowa, T. Balakier and J. Jurczak, Recognizing the Limited Applicability of Job Plots in Studying Host-Guest Interactions in Supramolecular Chemistry, *J. Org. Chem.*, 2016, **81**, 1746–1756.
30 M. J. Sabacky, C. S. Johnson, R. G. Smith, H. S. Gutowsky and J. C. Martin, Triarylmethyl Radicals. Synthesis and Electron Spin Resonance Studies of Sesquixanthydryl Dimer and Related Compounds, *J. Am. Chem. Soc.*, 1967, **89**, 2054–2058.
31 D. Shi, G. Sfintes, B. W. Laursen and J. B. Simonsen, Fluorescent and Highly Stable Unimodal DMPC Based Unilamellar Vesicles Formed by Spontaneous Curvature, *Langmuir*, 2012, **28**, 8608–8615.
32 D. Shi, C. Schwall, G. Sfintes, E. Thyrhaug, P. Hammershøj, M. Cárdenas, J. B. Simonsen and B. W. Laursen, Counterions Control Whether Self-Assembly Leads to Formation of Stable and Well-Defined Unilamellar Nanotubes or Nanoribbons and Nanorods, *Chem. – Eur. J.*, 2014, **20**, 6853–6856.
33 S. M. Ngola and D. A. Dougherty, Evidence for the importance of polarizability in biomimetic catalysis involving cyclophane receptors, *J. Org. Chem.*, 1996, **61**, 4355–4360.
34 H.-J. Schneider, Dispersive Interactions in Solution Complexes, *Acc. Chem. Res.*, 2015, **48**, 1815–1822.
35 D. A. Dougherty and D. A. Stauffer, Acetylcholine Binding by a Synthetic Receptor - Implications for Biological Recognition, *Science*, 1990, **250**, 1558–1560.
36 A. M. Agafontsev, T. A. Shumilova, A. S. Oshchepkov, F. Hampel and E. A. Kataev, Ratiometric Detection of ATP by Fluorescent Cyclophanes with Bellows-Type Sensing Mechanism, *Chem. – Eur. J.*, 2020, **26**, 9991–9997.
37 Y. Shiraishi, K. Ishizumi, G. Nishimura and T. Hirai, Effects of Metal Cation Coordination on Fluorescence Properties of a Diethylenetriamine Bearing Two End Pyrene Fragments, *J. Phys. Chem. B*, 2007, **111**, 8812–8822.
38 D. N. Laikov, A new parametrizable model of molecular electronic structure, *J. Chem. Phys.*, 2011, **135**, 134120.
39 F. Neese, The ORCA program system, *Wiley Interdiscip. Rev. Comput. Mol. Sci.*, 2012, **2**, 73–78.
40 A. M. Agafontsev, A. Ravi, T. A. Shumilova, A. S. Oshchepkov and E. A. Kataev, Molecular Receptors for Recognition and Sensing of Nucleotides, *Chem. – Eur. J.*, 2019, **25**, 2684–2694.